

Dependence of ion flow through the hemocyanin channel on a fixed charge at the pore mouth: effects of H^+ and Ca^{2+} ions

Gianfranco Menestrina * and Claudio Porcelluzzi

Dipartimento di Fisica, I-38050 Povo (TN) (Italy)

(Received March 1st, 1985)

(Revised manuscript received January 21st, 1986)

Key words: Ion channel; Hemocyanin; Voltage gating; pH control; Ion selectivity; Phospholipid bilayer

Incorporation of *Megatutura crenulata* hemocyanin into planar phospholipid bilayers results in the formation of ionic channels whose conductance can be directly measured. We have studied the effects of the pH on the electrical properties of these channels in the presence both of a K_2SO_4 solution, at high and low concentration, and of a KCl one. We have found that the conductance of the channel depends on the proton concentration following a positive titration curve, i.e., increasing sigmoidally with the pH at all the concentrations used; at any given pH, it additionally increases sublinearly with the concentration of the salt. The sublinear conductance-concentration dependence can be reverted to an almost linear one by the addition of suitable amounts of an indifferent cation such as tetramethylammonium to keep the ionic strength constant. The current-voltage curve of the channel, which is strongly voltage-dependent, is shifted along the voltage axis towards negative values by an increase in the proton concentration. Calcium ions have similar effects. The selectivity of the channel for cations over anions is strongly pH-dependent in the case of a KCl solution, being lost at pH 4.5, but is almost invariant in a K_2SO_4 solution. All experimental results are interpreted assuming the existence of a mechanism of voltage gating of the channel and of discrete negative charge fixed near its mouth. This charge can be neutralized by specific binding either of H^+ or of Ca^{2+} ions. The dissociation constants from the channel found for these two ions are consistent with those given in the literature for the hemocyanin protein and indicate that carboxyl groups and/or histidines are involved in forming the negative charge of the pore.

Introduction

Megatutura crenulata hemocyanin is a well-known and well-studied pore former. Despite the obscure physiological implications of this property, if any, it is now well established that hemocyanin, the oxygen transporter in many phyla of invertebrates, can form ionic channels through black lipid mem-

branes [1,2] as well as unilamellar liposomes of large size [3]. Morphological studies have indicated that *M. crenulata* assumes in the presence of lipid structures the shape of an annulus with an external diameter of about 7 nm and a central pool of stain roughly 2 nm wide, which is attached perpendicularly to the lipid surface and protrudes for about 3 nm into the external solution [4]. This structure is not commonly observed when the protein is in solution and is in fact supposed to be characteristic of the ionic pore.

The electrical properties of the pore have been extensively studied [5–8]; they include a sublinear

* To whom correspondence should be addressed.

Abbreviations: Bistris, 2-[bis(2-hydroxyethyl)amino]-2-(hydroxymethyl)propane-1,3-diol; Mes, 4-morpholineethanesulfonic acid.

conductance-concentration relationship, cation selectivity and voltage dependence and make this pore an interesting model of natural channels occurring in excitable cells. We have previously proposed a model for this channel which couples free diffusion through the pore, of the type given by the Goldman-Hodgkin-Katz (GHK) equation, with the effects of a negative charge fixed on the channel which produces a local ion concentration quite different from that of the bulk [7,8]. On the other hand, Cecchi et al. [5,6] have proposed a single-file single-ion occupancy three-barrier two-site model of the channel which could also predict its electrical properties. To test whether our hypothesis of a negative fixed charge on the pore is tenable, we have now studied extensively the effects of the pH upon the conductance of the channel, both at high and low concentrations. As pointed out by Lindemann [9], a channel obeying the GHK equation with titratable fixed charges at its mouth is always expected to show a positive titration curve, i.e., its conductance should increase with the pH, while a multibarrier multisite pore is expected to show a positive titration curve at low channel occupancy but a negative one at high values of channel occupancy, i.e., in the region of saturation. We have indeed found a positive titration curve of the hemocyanin channel conductance at all the concentrations used (0.01–0.5 M) and with different electrolytes, confirming the idea of a fixed charge being present and of GHK diffusion.

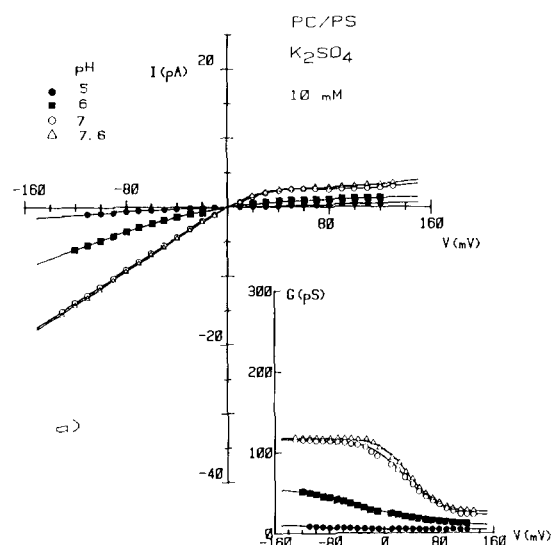
We have also found that the selectivity of the channel for cations over anions decreases upon decreasing the pH in the case of KCl and is lost at pH 4.5, i.e., near the isoelectric point of the protein. Similar behavior has been observed previously by others studying the channel formed by porin, the matrix protein from the outer membrane of *Escherichia coli*, and attributed also in that case to the presence of a negative fixed charge on the pore [10,11]. We can show here that our model can be successfully used to describe the pH and also the Ca^{2+} -dependence of the channel properties, assuming that the negative charge is composed of binding sites for protons and divalent cations.

We have estimated the dissociation constants for these two ions and found $\text{p}K_{\text{H}^+} = 5.4$ and $\text{p}K_{\text{Ca}^{2+}} = 2.4\text{--}2.7$. It is worth noting that a similar

pH and Ca^{2+} control has been observed in the gap junctional conductance and that dissociation constants ranging $\text{p}K_{\text{H}^+} = 7.3$ and $\text{p}K_{\text{Ca}^{2+}} = 3.25\text{--}3.45$ have been estimated for this natural channel [12,13]. Even more similar dissociation constants, $\text{p}K_{\text{H}^+} = 5.8$ and $\text{p}K_{\text{Ca}^{2+}} = 2.0\text{--}2.6$, have been measured by Kostyuk and co-workers [14], studying the Ca^{2+} channel of the mollusc neuron membrane. We think that, once more, the hemocyanin channel proves to be a valuable tool with which to explore general mechanisms of transport which can be shared by other physiological systems.

Materials and Methods

Black lipid membranes were prepared by the usual technique [15] on a circular hole, 0.5 mm in diameter, drilled in a Teflon septum separating two aqueous solutions. The lipids used were either saturated egg phosphatidylcholine (PC) more than 99% pure, purchased from P.L. Biochemicals, or a mixture of this phosphatidylcholine with bovine brain phosphatidylserine, Gold Label from Calbiochem, PC/PS 2:1 (w/w); both lipids were dissolved in *n*-decane to a final concentration of 45 mg/ml. Electrolytes were prepared from twice-distilled water using the best grade reagents available from Carlo Erba, they were buffered either by 5 mM Tris- H_2SO_4 for pH values ranging from 6 to 8 (buffer A), by 5 mM Mes-KOH, for pH 4–6 (buffer B), or by 10 mM Bistris-HCl in the experiments where chloride salts were used (buffer C). Tris, Mes and Bistris were all purchased from Calbiochem. Small amounts of EDTA were also present to eliminate traces of divalent cations, which strongly interact with the channel [7]; in the experiments with CaSO_4 the concentration of Ca^{2+} given is that in excess of the EDTA present. *M. crenulata* hemocyanin, Calbiochem A grade, nominally 100 mg/ml, was stored at -20°C in 50% glycerol. Before each experiment it was diluted to 10 mg/ml and dialysed overnight against the bath solution. Small amounts of this sample were added to one compartment only, cis side, at least 15 min after complete blackening of the membrane, to a final concentration ranging from 1 to 10 $\mu\text{g/ml}$, depending on the concentration and the pH of the solution. Two Ag|AgCl electrodes were used to apply voltage and to measure membrane current;



they were connected to the solutions through agar bridges containing 2 M KCl. Current flowing through the membrane was converted to voltage by a virtual ground operational amplifier (AD 515 K) with a $1 \cdot 10^8 \Omega$ resistor in parallel to a 2 pF capacitor in the feedback loop, and recorded on a $x-t$ strip chart recorder. Applied voltages, which were clamped by the virtual ground configuration, had the cis compartment as the reference, and currents were defined positive when cations flowed into the same compartment. Experiments were performed at room temperature.

Single channel conductance was evaluated by the height of the current steps observed at a fixed voltage (usually -40 mV) during the incorporation of the first 10–60 channels. Instantaneous current-voltage curves were obtained applying short-lived voltage pulses (duration 0.3–0.5 s) of different amplitudes, starting from a zero resting potential. The rationale for these procedures and the corrections needed to take into account the formation of new channels during the measure have been fully described in previous works [7,8]. Several (2–5) I/V curves were recorded during each experiment and then averaged. The experiments were repeated two to four times. Selectivity experiments were performed as follows: a black lipid membrane was prepared separating two symmetrical, low-concentration solutions; the concentration of the trans compartment was then raised and hemocyanin was added to the cis com-

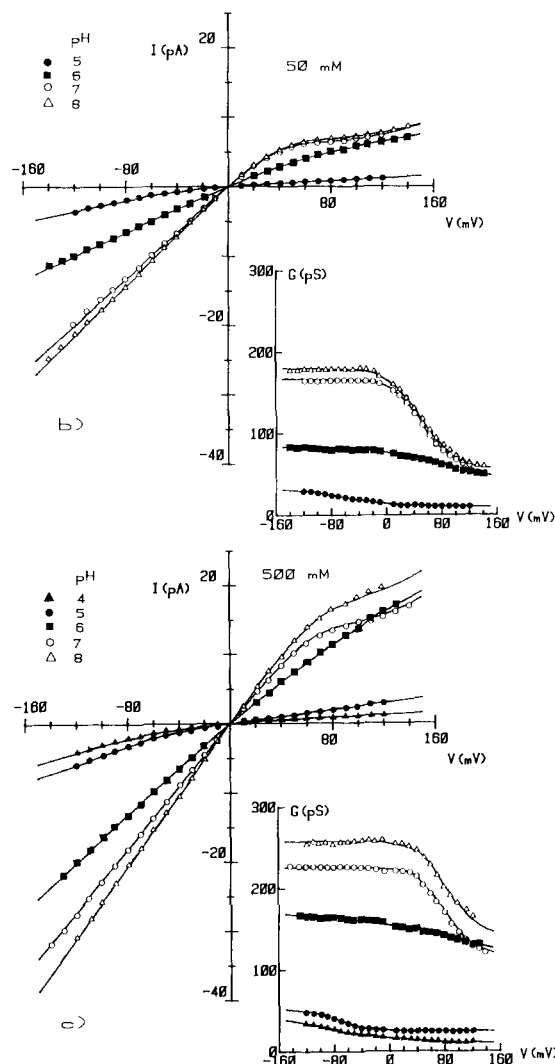


Fig. 1. Instantaneous current-voltage curves of a hemocyanin channel at different pH values of the solution. In the inset are shown the corresponding conductance-voltage curves. Symmetrical solutions containing different K_2SO_4 concentrations have been used: (a) 10 mM, (b) 50 mM and (c) 500 mM; they were buffered using either buffer A (open symbols), or buffer B (closed symbols). Membranes were comprised of a 2:1 PC/PS mixture. Each curve is the mean of 2–5 I/V tests obtained during the same experiment. Solid lines are drawn according to the two-state model, Eqns. 1 and 2, with $I = G \cdot V$. The values of the four parameters GA , GB , z_g and V_0 for a best fit were found by a least-squares procedure and used to build up Figs. 2, 3 and 8.

partment; voltage ramps were applied to the membrane and the I/V curve was recorded on a $X-Y$ plotter during the incorporation of the protein;

curves recorded at successive times had increasing slopes due to the insertion of new channels during the course of the experiment; their intercept indicated the point at which $I = 0$. The abscissa of this point, with respect to that in the absence of the membrane, obtained by breaking the black lipid membrane at the end of the experiment, was called the reversal or zero-current potential.

Results

Instantaneous current-voltage (I/V) curves of hemocyanin-doped membranes bathed by a symmetrical K_2SO_4 solution are shown in Fig. 1 as a function of the pH and for three different concentrations of the electrolyte. The I/V curves have been obtained with membranes containing many channels, but for the presentation in the figure they have been scaled to the current that would flow through a single channel, making use of the single-channel current measured at a fixed voltage by the height of the incorporation steps. The pro-

cedure to obtain these I/V curves is given in Materials and Methods and has been described in great detail in previous works, also [7,8]. Each I/V curve is markedly non-linear and is also pH-dependent; in fact, increasing the pH has the effect of increasing the slope of the curve in the negative voltage region. This behavior is qualitatively the same at all three K_2SO_4 concentrations, but comparing curves at the same pH one can notice that the slope in the third quadrant increases also upon increasing the electrolyte concentration. Conductance-voltage (G/V) curves corresponding to the same experiments are shown in the inset of each panel. The G/V curves show in each case a typical sigmoidal shape, which allows us to extrapolate two asymptotical conductance values for the hemocyanin channel, one for high negative voltages, which we call G_A , and one for high positive potentials, G_B . One can see from Fig. 1 that both these values decrease when the pH is decreased at a constant K_2SO_4 concentration, and that they increase with the salt concentration at a constant

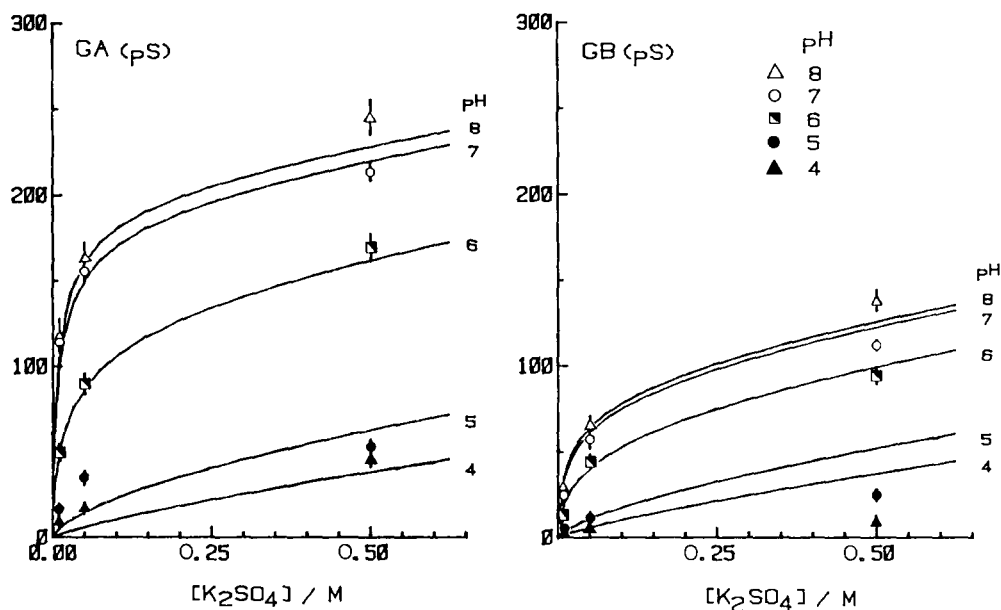


Fig. 2. High and low conductance of the hemocyanin channel, G_A and G_B , obtained extrapolating from the G/V curve at high negative and high positive applied voltages, respectively. They are plotted as a function of the K_2SO_4 concentration for different values of the pH of the solution. Each point is the mean value \pm S.D. out of 2–4 different experiments like those shown in Fig. 1. Buffers used were either buffer A, (open symbols) or buffer B (closed symbols). Half-filled symbols are means of experiments done with both buffers. Membranes were comprised of the PC/PS mixture. Solid lines are drawn according to the electrostatic model, Eqns. 3 to 8. The values of the parameters which have been used are: $\pi r^2/l = 3$ pm; $a(A) = 0.41$ nm; $a(B) = 0.53$ nm; $N = 3.8$; $pK_{H^+} = 5.4$.

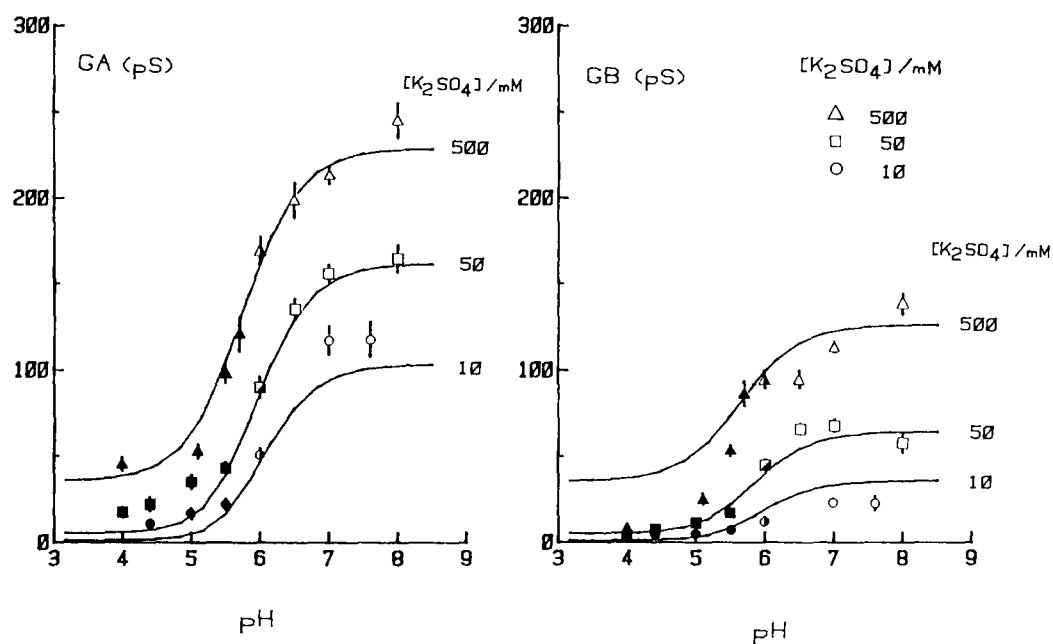


Fig. 3. High and low conductance of the hemocyanin channel, G_A and G_B respectively, as a function of the pH of the solution at different values of the K_2SO_4 concentration. Open, half-open and closed symbols and all other experimental conditions as for Fig. 2. Solid lines are drawn according to Eqns. 3–8 with the parameters given in Fig. 2.

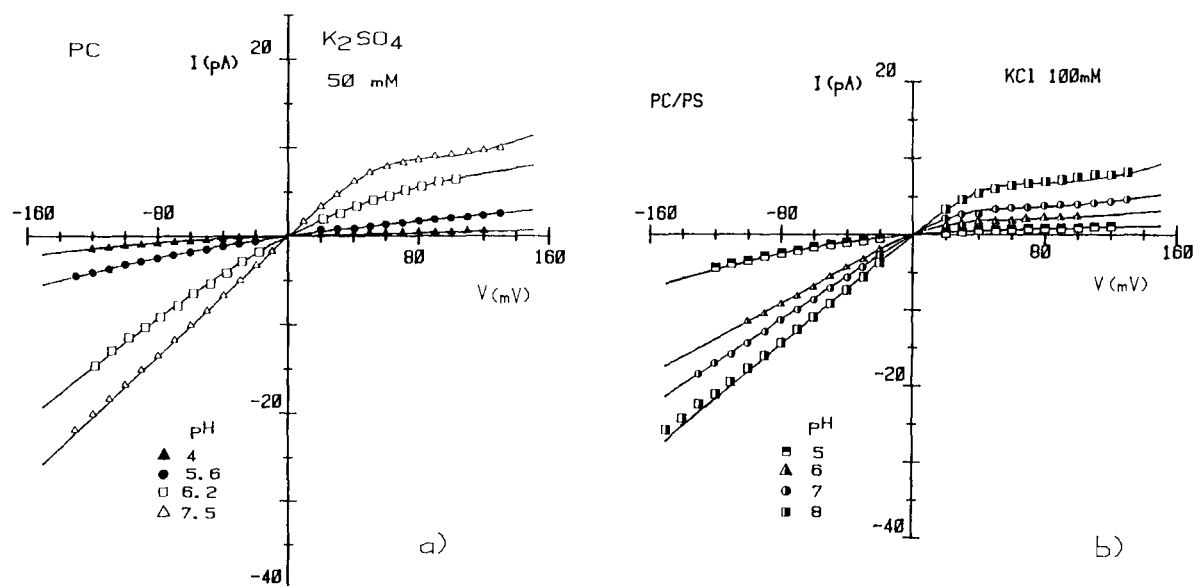


Fig. 4. Instantaneous I/V and G/V curves of a hemocyanin channel. (a) Experimental conditions as for Fig. 1b, except that membranes were comprised of pure PC. Open and closed symbols for buffers A and B, respectively. (b) Same as part a but using 100 mM KCl buffered by buffer C as bathing solution. Membranes were comprised of PC/PS. Solid lines in both parts are least-squares adaptations of Eqns. 1 and 2, and the parameters found are plotted in Figs. 5 and 9.

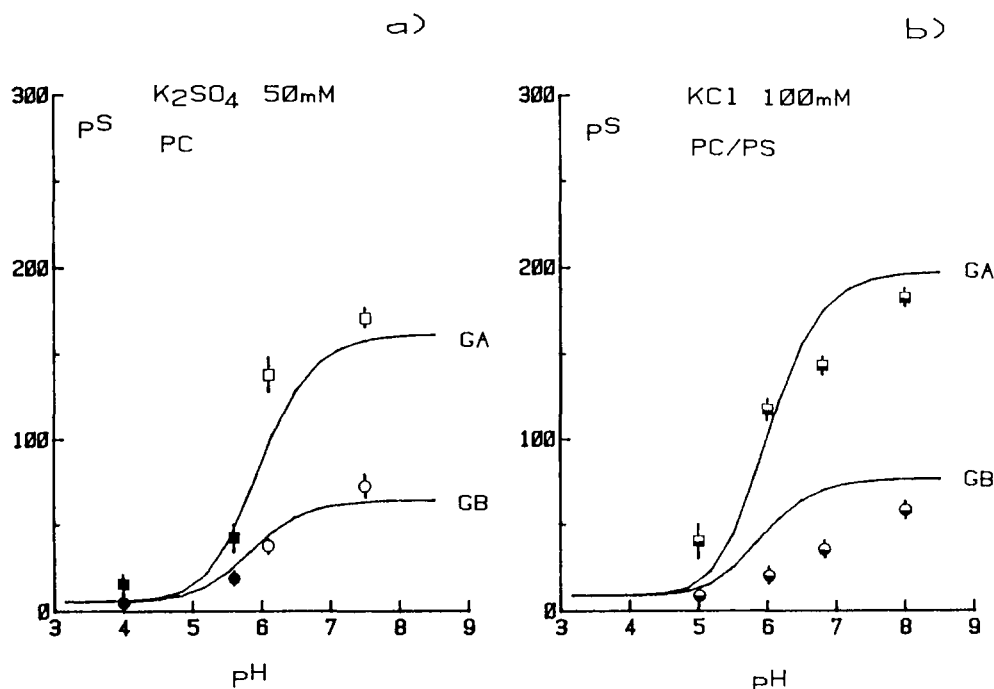


Fig. 5. High and low conductance of the hemocyanin channel, G_A and G_B , respectively, as a function of the pH of the solution either for a PC membrane bathed by 50 mM K_2SO_4 (a) or for a PC/PS membrane bathed by 100 mM KCl (b). Experimental conditions are the same as for Fig. 4. Solid lines are drawn according to the electrostatic model, Eqns. 3–8, with the parameters reported in Fig. 2.

pH. The values of G_A and G_B are shown in Fig. 2 as a function of K_2SO_4 concentration for different pH values. Both increase nonlinearly with the concentration, showing a decreasing slope; in all cases, the conductance is higher, the higher the pH. Conversely, in Fig. 3 we have presented the same two quantities as a function of the pH, for the three concentrations used. At all salt concentrations they show a sigmoidal dependence on the pH of the solution which is reminiscent of a simple titration curve. The experiments presented until now have been performed using membranes comprised of a PC/PS mixture, which are negatively charged. To investigate whether the black lipid membrane surface charge has an effect on the hemocyanin channel conductance, we have repeated the experiments at the intermediate concentration also using membranes comprised of pure PC, which should be neutral. I/V and G/V curves obtained in this way at different pH values are shown in Fig. 4a. They follow the same qualitative behavior of the preceding experiments, and a comparison with Fig. 1, panel b, indicates that no

substantial change is introduced by the surface charge of the membrane. As a control, the same type of experiments have been performed also with a KCl solution (Fig. 4b) using PC/PS membranes, to investigate the possible effects of the different anion. Once more, S-shaped G/V curves resulted and the conductance was shown to be dependent on the pH of the solution, decreasing when this was decreased at every applied voltage. The two asymptotical conductance values, G_A and G_B , are reported in Fig. 5 both for the case of a the K_2SO_4 solution with neutral, PC, membrane and for the case of the KCl solution with the charged, PC/PS, membrane as a function of the pH. In all cases, they depend on the pH in a way which is quite similar to that already shown in Fig. 3.

In order to understand the role of the ionic strength in determining the conductance-concentration relationship we have studied the hemocyanin channel in PC membranes at a fixed pH (7.0) in the presence of varying amounts (0.01–0.2 M) of K_2SO_4 either alone or with the addition of

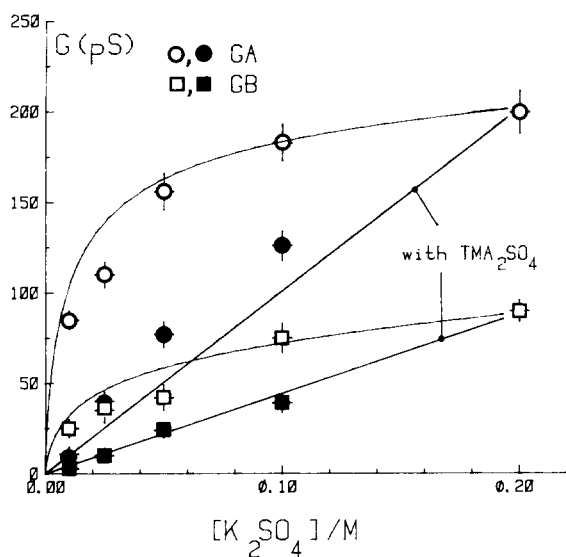
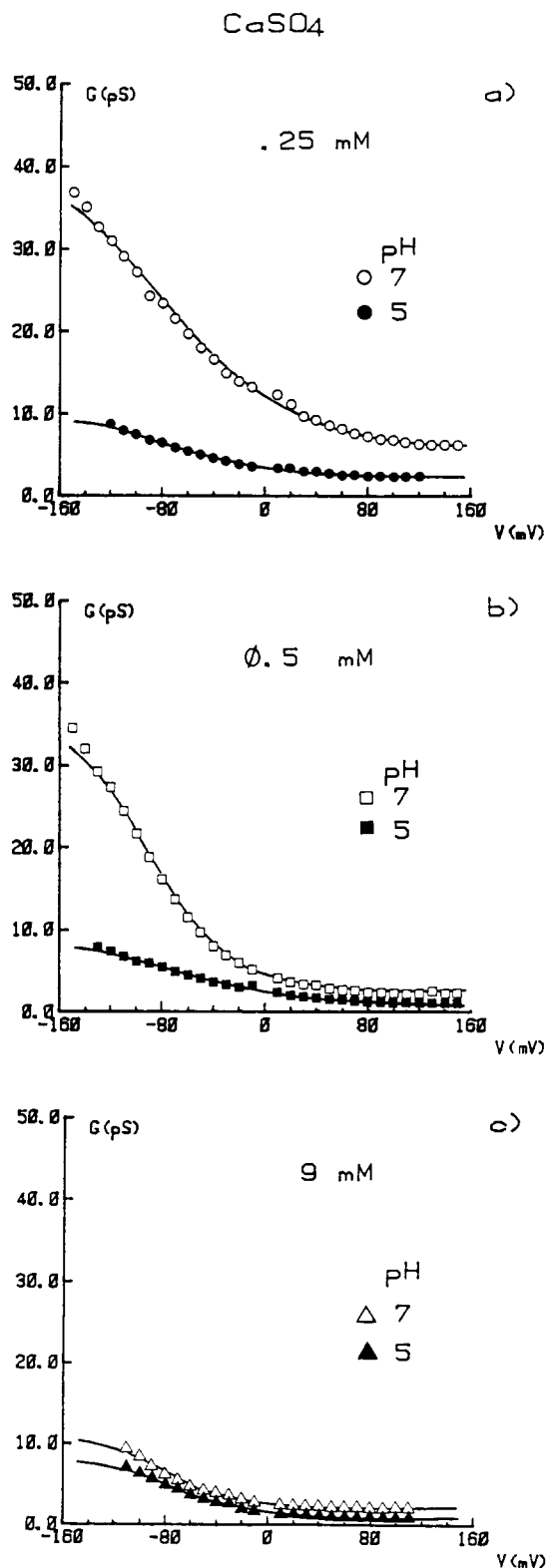


Fig. 6. High and low conductance of the hemocyanin channel, GA (circles) and GB (squares) as a function of the K_2SO_4 concentration either in buffer A alone, empty symbols, or in buffer A plus amounts of tetramethylammonium sulfate to keep the SO_4^{2-} concentration constant at 0.2 M (filled symbols). Membranes were comprised of pure PC, other experimental conditions as in Fig. 2. Solid lines are drawn according to the electrostatic model, Eqns. 3–8, with the parameters listed in the legend of Fig. 2.

enough tetramethylammonium sulfate to keep constant the SO_4^{2-} concentration to 0.2 M. Tetramethylammonium sulfate has been chosen because both ion species in this salt are almost impermeant through the channel; we have indeed measured a maximum pore conductance of 5 pS in the presence of 0.2 M tetramethylammonium sulfate, in good agreement with the value of 1.8 pS reported by Cecchi et al. [16] for the case of 0.05 M tetramethylammonium sulfate. The results of these experiments are shown in Fig. 6. As in the case of PC/PS membranes, the conductance concentration curve is strongly sublinear in the presence of

Fig. 7. Instantaneous G/V curves of a hemocyanin channel under the same experimental conditions as in Fig. 1a, but with different amounts of $CaSO_4$ added symmetrically to the bathing solutions: (a) 0.25 mM; (b) 0.5 mM; (c) 9 mM and for two values of the pH: 5.0 and 7.0. Open symbols, buffer A; closed symbols, buffer B. Solid lines are least-squares fit of the two-state model, Eqns. 1 and 2; the best fit parameters are plotted in Fig. 10.



K_2SO_4 alone, but is converted to an almost linear one by the addition of the indifferent cation, tetramethylammonium.

In order to see whether the pH can also affect the selectivity of the channel between anions and cations, we have measured the reversal potential of hemocyanin-doped membranes placed between asymmetrical solutions both of K_2SO_4 and of KCl at different pH values. The results, obtained following the procedure given in materials and Methods, are reported in Table I. A negative voltage, corresponding to a substantial cation selectivity, has been measured in the case of the K_2SO_4 solution, which was almost independent of the pH, whereas in the case of the KCl solution a negative value was found at pH 7.0 but decreased upon decreasing the pH, becoming practically zero at pH 4.5. Finally, we have performed experiments adding small amounts of $CaSO_4$ to a 10 mM K_2SO_4 solution in which PC/PS membranes have been prepared. We have then added hemocyanin and we have recorded single-channel conductance and instantaneous I/V curves. The relative G/V curves, normalized to the single-channel conductance, are shown in Fig. 7 for three different Ca^{2+} concentrations. It was found that even small amounts of Ca^{2+} can depress the channel conductance, for example, 0.25 mM Ca^{2+} reduces the maximal conductance of the channel to about one-third of its normal value (compare Figs. 1 and 9). Even when divalent cations are present, the pH exerts its control on the channel conductance, as can be seen comparing the G/V curves obtained at pH 7.0 and those at pH 5.0: in all cases the conductance is lower the lower the pH.

Discussion

To explain the nonlinearity of the I/V curve of the hemocyanin channel and its dependence on the composition of the bathing solution, a model has been previously proposed by us [7] which assumes that the channel bears a negative fixed charge near its mouth, that it possesses two conformations in an electric field and that ions diffuse freely through it. The model has then been completed [8], in order to explain the effects of Tb^{3+} and Ca^{2+} , which are well known ligands of this protein, including in it the possibility of specific

binding of certain cations to the channel. We will show here that this same model, after proper adaptations, can explain also the findings presented in this paper.

The two-state model

The first assumption we make, in order to explain the sigmoidal shape of the G/V curve of the pore, as shown in Fig. 1, is that the channel can be described by a simple two-state gating model, of the type discussed, for example, in Ref. 17; in this case the conductance, G , of the channel can be written:

$$G(V) = G_B + [G_A - G_B]p(V) \quad (1)$$

with

$$p(V) = 1/[1 + \exp(z_g e(V - V_0)/kT)] \quad (2)$$

where G_A and G_B are the conductances of the channel in the states A and B, respectively, z_g is the valence of the gating charge, e is the elementary charge, V the applied voltage, p represents the probability of occupancy of state A, and V_0 is the inflection voltage of the sigmoidal conductance, i.e., the potential at which $p = 1/2$.

We have used a two-state model for the channel even if we could not resolve discrete fluctuations between the two conformations because, as pointed out by Lauser [18], proteic channels are able to undergo very fast conformational transitions, with lifetimes in the picosecond to nanosecond range, well beyond the time resolution of electrophysiological measurements. In such a case, only a time-averaged conductance can be observed at any applied voltage.

We have fitted our experimental G/V curves to Eqns. 1 and 2 and we have obtained the best values of the four parameters G_A , G_B , z_g and V_0 by a least-squares procedure. It is found that all these parameters depend upon the electrolyte composition, i.e., pH, concentration and ionic composition of the solution. It is our aim in the following to discuss these variations and to describe them in terms of simple models.

G_A and G_B : the electrostatic model

As we have previously indicated [7,8], the cation selectivity, see Table I, sublinear conductance-con-

centration curve (Fig. 2) and pH-dependence (Fig. 3) of the hemocyanin channel suggest that a negative charge fixed on the protein plays an important role in its conductance properties. We can consider the channel as a cylindrical pore of radius r and length l filled with aqueous solution where ions can move as in the bulk, but whose mouths are placed at the surface of a macroion, the channel itself, which bears a net fixed charge, Q . In this case, we have a concentration of ions at the pore mouth which is quite different from that in the bulk, counterions being in large excess over coions. Accordingly, the channel conductance can be written as [19]:

$$G_{\alpha} = \sum_i G_i(\alpha) = \sum_i \frac{\pi r^2}{l} w_i z_i e C_{iL}(\alpha) \gamma_{iL}(\alpha) \quad (3)$$

where the index i identifies all the ion species present in the solution, the final conductance being the sum of the contributions due to each ion species; r and l have been defined above; w_i and z_i are the conventional mobility and the valence of the ion species i ; C_{iL} and γ_{iL} are the local concentration and local activity coefficient of the ion i at the pore mouth. The index, α , can be A or B, and consistently Eqn. 3 represents the conductance of the channel in state A or B.

TABLE I
HEMOCYANIN CHANNEL SELECTIVITY

Reversal potential, V_{rev} , of the hemocyanin channel under asymmetrical solution conditions; trans-side activity higher than the cis-side one. Experiments were performed using PC/PS membranes bathed either by K_2SO_4 , two left-hand columns, or by KCl, the right-hand columns. Experimental (exp) values were measured as indicated in Materials and Methods, whereas theoretical (theo) values have been calculated according to the electrostatic model, by Eqn. 9, making use of the parameters listed in Fig. 2. The reversal potential corresponding to an ideal cation selectivity would have been -34.8 mV for the K_2SO_4 solution and -49.5 mV for the KCl one. The buffer used is indicated.

Buffer	pH	K_2SO_4		KCl	
		$(V_{\text{rev}})_{\text{exp}}$	$(V_{\text{rev}})_{\text{theo}}$	$(V_{\text{rev}})_{\text{exp}}$	$(V_{\text{rev}})_{\text{theo}}$
A	7.0	-32 ± 1	-34.8	-36 ± 2	-46.5
A, B	5.8	-30 ± 2	-34.2	-22 ± 3	-39.6
B	4.5	-27 ± 3	-31.1	2 ± 3	-10.8

To evaluate the local concentration of the ion species i , i.e., C_{iL} , one has to take into account the surface potential due to the channel charge, which we call ψ_L , hence:

$$C_{iL}(\alpha) = C_{io} \exp(-z_i e \psi_L(\alpha) / kT) \quad (4)$$

where C_{io} is the bulk concentration of the ion i , k and T have their usual meaning and the other symbols have been defined above. The local activity coefficient, γ_{iL} , has also to be evaluated for each ion species. To this purpose we have used a published general expression for the activity coefficient of single ion species which is valid up to very high concentrations, i.e., eqn. 89 in Ref. 20. According to recent studies on counterion condensation at the surface of polyelectrolytes [21,22], we have introduced the local ionic strength, defined as:

$$I_1 = \frac{1}{2} \sum_i C_{iL} z_i^2 \quad (5)$$

into the expression for the activity coefficient, to achieve a more realistic value.

The potential, ψ_L , can be calculated using the simplest possible expression for it, i.e., the Debye-Hückel potential at the surface of a macroion of charge Q [23]:

$$\psi_L(\alpha) = \frac{Q}{4\pi\epsilon} \frac{1}{(1 + \chi a(\alpha)) \cdot a(\alpha)} \quad (6)$$

where ϵ is the dielectric constant of water, χ the Debye-Hückel coefficient and a is the closest possible approach distance between the ions of the solution and the charge of the macroion. We have allowed the parameter a to be different in the two states A and B, since they correspond to two different conformations of the channel. The use of the Debye-Hückel expression for the potential, Eqn. 6, may be questioned, since we are dealing with large local potentials and high local concentrations. Nevertheless, one should notice that, despite the severe approximations used to derive it, the Debye-Hückel potential has proved to give quite accurate predictions on the properties of electrolytic solutions when compared to recently developed exact theories, even at very high bulk concentrations [24] as well as at high local potentials. Furthermore, we feel that a search for a

better expression for the potential, though possible, is unnecessary for the point to be made here, i.e., that sublinear dependence on the salt concentration, selectivity and pH-dependence of the hemocyanin channel conductance can be explained by a negative charge fixed on it.

The decreasing slope of the conductance-concentration relation arises in this model by the screening effects of counterions, that is by the presence of the coefficient χ , which is proportional to the square root of the ionic strength I_L [19] at the denominator of Eqn. 6. In fact, increasing the concentration of the salt decreases the potential ψ_L and hence, through Eqn. 4, it decreases the counterion accumulation and the conductance of the channel with it. The fixed-charge model predicts that the conductance-concentration relation becomes linear at very high concentrations. This is exactly what we have observed in a previous work using high concentrations of monovalent cations [7]. Additional evidence for the fixed-charge model comes from the experiment in Fig. 6, where it is shown that buffering the ionic strength with an indifferent cation such as tetramethylammonium has also the effect of linearizing the conductance-concentration curve.

We introduce now the pH-dependence in the conductance, G , just by assuming that the fixed charge, Q , on the channel is composed of a certain number of equal sites which can bind protons from the solution becoming neutralized. In this case we have:

$$Q = Q_{\text{tot}} / (1 + [H^+] / K_{H^+}) \quad (7)$$

with

$$Q_{\text{tot}} = -N \cdot e \quad (8)$$

where N is the number of negative monovalent sites, e is the elementary charge and K_{H^+} is the dissociation constant of the proton from the sites. Combining now Eqns. 3–8 it is possible to calculate the conductance of the channel in both states A and B as a function of the pH and of the salt concentration for a given set of the model parameters. This has been done, and by matching computer-generated theoretical lines with the experimental points of Figs. 2 and 3, we have found that

it is possible to describe the hemocyanin channel properties at best with the following choice of the parameters: $\pi r^2/l = 3$ pm; $a(A) = 0.41$ nm; $a(B) = 0.53$ nm; $N = 3.8$; $pK_{H^+} = 5.4$. It is worth discussing briefly here the parameter values that we have found. The geometrical factor, $\pi r^2/l$, indicates a pore radius of about 1 Å, assuming a channel length of 10 nm (a plausible length, since the channel protrudes about 3 nm at least in the cis solution [4]); this radius is less than that found by pore size analysis by Cecchi et al. [16], which was 2.1–2.4 Å; this discrepancy probably indicates only that the mobility, W_i , of ions into the channel is somewhat restricted compared to the bulk solution value we have used in eqn. 3. The two Debye-Hückel parameters, $a(A)$ and $a(B)$, are both in the range typical for electrolytes i.e., 3–5 Å, and differ one from the other by merely 1.2 Å, indicating a small rearrangement of the sites upon the conformational transition of the protein.

Interestingly enough, Brooks and Karplus [25] have shown recently that displacements of 1–2 Å at a number of residues along the lysozyme peptide chain occur with a frequency in the range of 10^{11} Hz. This provides the basis for our assumption that conformational transitions between the two states of the pore can occur so quickly that only an average conductance can be measured. The value of N indicates that the total charge influencing the mouth of the channel is composed by something like four sites of valence -1 . The presence of a negative charge on the channel is a highly tenable hypothesis, since it is known that hemocyanin is a negatively charged molecule at pH > 4.4 [26]. The pK_{H^+} value found will be discussed in detail at the end of this section.

Since the pore entrance is located at least 3 nm apart from the black lipid membrane surface and in the center of a 7 nm diameter proteic ring [4], it is not likely that it is influenced by the charge of the membrane. Hence we may suppose that the parameters we have found can describe the channel conductance also when neutral membranes are used. That this is the case is shown in Fig. 5, part a, and Fig. 6, empty symbols. Furthermore, the same set of parameter values can describe also the pH dependence of the channel conductance in the presence of KCl, as shown in Fig. 5, part b, as

well as the linearizing effects of the impermeant cation tetramethylammonium presented in Fig. 6, filled symbols. This means that our model, with the parameter values optimized for K_2SO_4 solutions and PC/PS membranes, can be successfully used to predict the results of control experiments performed using completely different solution and membrane compositions.

Cation selectivity of the channel arises in this model by the fact that cations, which are the counterions, are attracted to the negatively charged pore, while anions, which are the coions, are repelled from it. Using a very general expression for the reversal potential, V_{rev} , as obtained from the Goldman-Hodgkin-Katz equation [27] we can write:

$$V_{rev} = \frac{e}{kT} \sum_i \left(\left(\frac{G_i}{\sum_j G_j} \right) \frac{1}{z_i} \ln \frac{a'_i}{a''_i} \right) \quad (9)$$

where G_i is defined by Eqn. 3 and the summations are extended to all ion species present; a'_i and a''_i are the activities of the ions i in the solution at the cis and trans side, respectively; the other symbols have been already defined. Using Eqns. 3–8 we can calculate the values of G_i and, by Eqn. 9, with the appropriate values of a_i the reversal potential V_{rev} . Table I indicates that our model, with the same parameters listed above, not only predicts almost exactly the reversal potential found in the K_2SO_4 solution, for which the parameters have been optimized, but also reproduces at least qualitatively the pH dependence of V_{rev} in the KCl solution, though a shift of about -10 mV is observed between theoretical and experimental values.

Finally, Eqn. 7 can easily be extended to the case that divalent cations bind to the same sites as protons on the channel, in order to explain the Ca^{2+} effects shown in Fig. 7. Assuming that one Ca^{2+} ion can neutralize two monovalent sites at a time, because of its double charge, we have:

$$Q = Q_{tot} / (1 + [H^+] / K_{H^+} + [Ca^{2+}] / K_{Ca^{2+}}) \quad (10)$$

where the dissociation constant for the binding of Ca^{2+} ions, $K_{Ca^{2+}}$, has been introduced. With this extension the model can be used to describe the

channel conductance as a function of Ca^{2+} concentration and pH as shown in Fig. 10, upper parts, just with the addition of one new parameter, i.e., the Ca^{2+} dissociation constant, which was found to be $K_{Ca^{2+}} = 4$ mM.

z_g and V_0 , the four-state model

To explain the dependence of the other two parameters of the gating model, z_g and V_0 , on the pH of the solution we have to generalize the two-state model. This can be done, following Hanke and Miller [28], assuming the presence on the protein of an additional binding site for protons whose affinity changes during the transition of the channel between the two states A and B, but whose occupancy does not modify the conductance of each state. This site is not necessarily near the ion pathway but must be accessible from the solution. As we have already shown [8], this results in the introduction of a four-state model:



where K_{AH^+} , K_{BH^+} are dissociation constants of the protons from the channel in state A and B, respectively, and K_2 , K_1 are equilibrium constants for the conformational transition of the pore between the two configurations when protons are and are not bound to the site, respectively. Calling $p(V)$ the probability of the channel to be in one of the electrically indistinguishable A states, one can write:

$$\frac{p(V)}{1-p(V)} = K_1 \frac{(1 + \{[H^+] / K_{AH^+}\}^n)}{(1 + \{[H^+] / K_{BH^+}\}^n)} \quad (12)$$

where we have introduced a Hill coefficient, n , to allow for cooperative binding of more than one proton to the site. In general, the equilibrium constants can be voltage-dependent:

$$K_i(V) = K_i(0) \exp(-q_i V / kT) \quad (13)$$

where i can be 1, 2, A or B and q_i has the meaning of a true gating charge when $i = 1, 2$, whereas it can be written as

$$q_i = z\delta_i \quad (14)$$

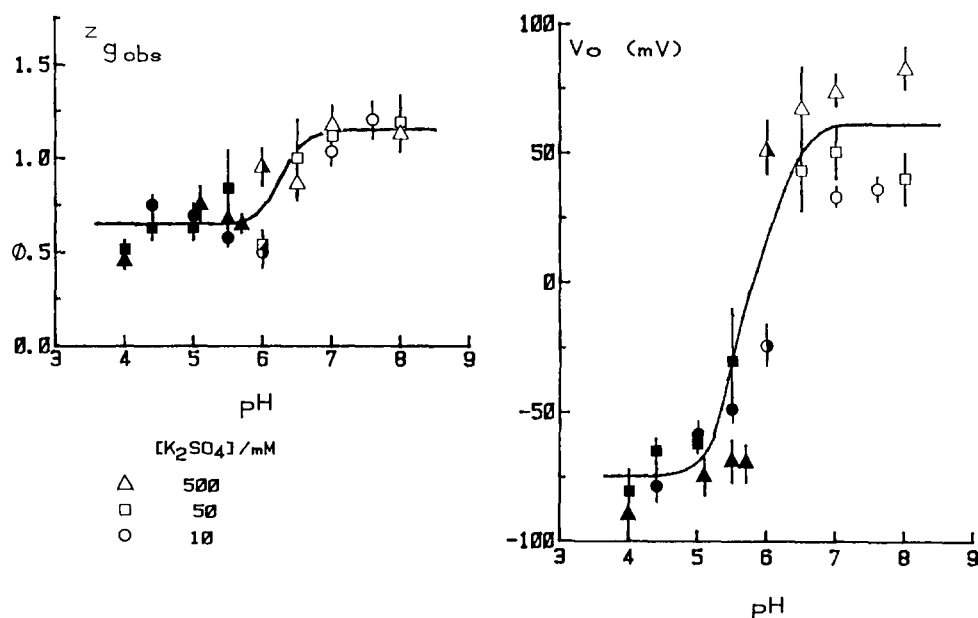


Fig. 8. Slope, $z_{g,obs}$, and inflection point, V_0 , of the G/V curve of the hemocyanin channel as a function of the pH of the solution for three different K_2SO_4 concentrations. Each point is the mean of 2–4 experiments like those presented in Fig. 1. Solutions were buffered with buffer A (open symbols) or buffer B (closed symbols); experiments were done with both buffers in the case of half-filled symbols. Other experimental conditions as in Fig. 1. Solid lines are solutions of Eqns. 15 and 16 for the four-state model using the following parameter values: $n = 2$; $K_1(0) = 14.9$; $Z_1 = 1.15$; $pK_{AH^+}(0) = 5.4$; $\delta_A = 0$; $pK_{BH^+}(0) = 6.4$; $\delta_B = -0.25$.

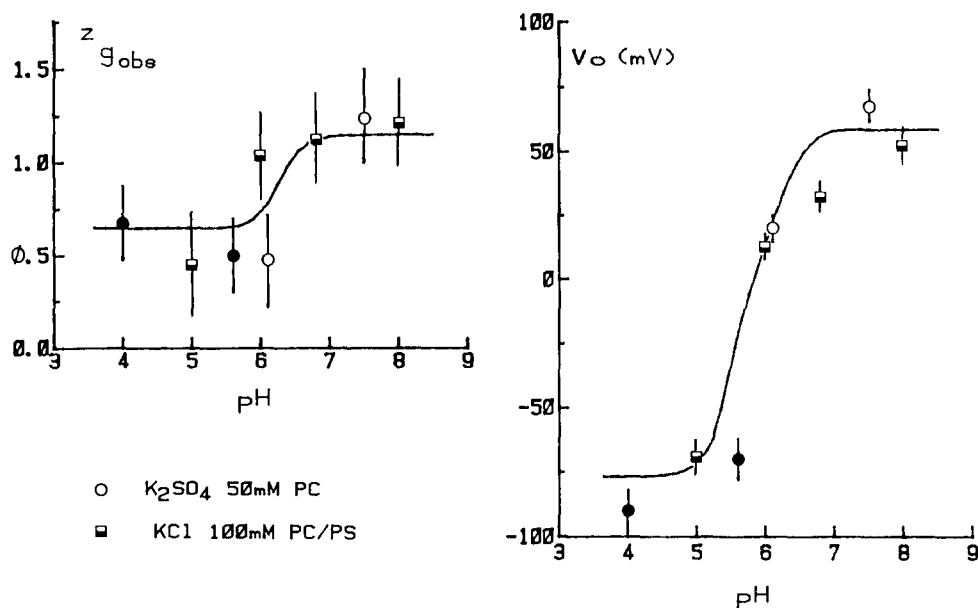


Fig. 9. Slope and inflection point, $z_{g,obs}$ and V_0 , respectively, of the G/V curve of the hemocyanin channel as a function of the pH of the solution either for a PC membrane bathed by 50 mM K_2SO_4 , circles, or for a PC/PS membrane bathed by 100 mM KCl, squares. Experimental conditions are the same as given in Fig. 4. Solid lines are the same as in Fig. 8.

for the case $i = A, B$, with z , the valence of the binding ion and δ_i the fraction of the potential felt by the ion at the binding site in the configuration i .

According to Ref. 28, an apparent gating charge can be calculated also for this model, whose valence is given by:

$$z_{g,obs} = -\frac{kT}{e} \left[\frac{d}{dV} \ln \left(\frac{p}{1-p} \right) \right]_{V=V_0} \quad (15)$$

and finally the voltage V_0 of the inflection point can be calculated resolving eq. 12 with $p = 1/2$:

$$1 = K_1(V_0) \frac{(1 + \{[H^+]/K_{AH^+}(V_0)\})^n}{(1 + \{[H^+]/K_{BH^+}(V_0)\})^n} \quad (16)$$

Analytical solutions for $z_{g,obs}$ and V_0 are not easily found for the general case, but, as we have already discussed, it is possible to find some useful approximations with wide ranges of applicability [8,29]. Using these approximations we have generated the solid lines in Fig. 8 and we have compared them with the experimental data for the K_2SO_4 solutions at different concentrations. We have found that a good fit is obtained with the following choice of the model parameter: $n = 2$;

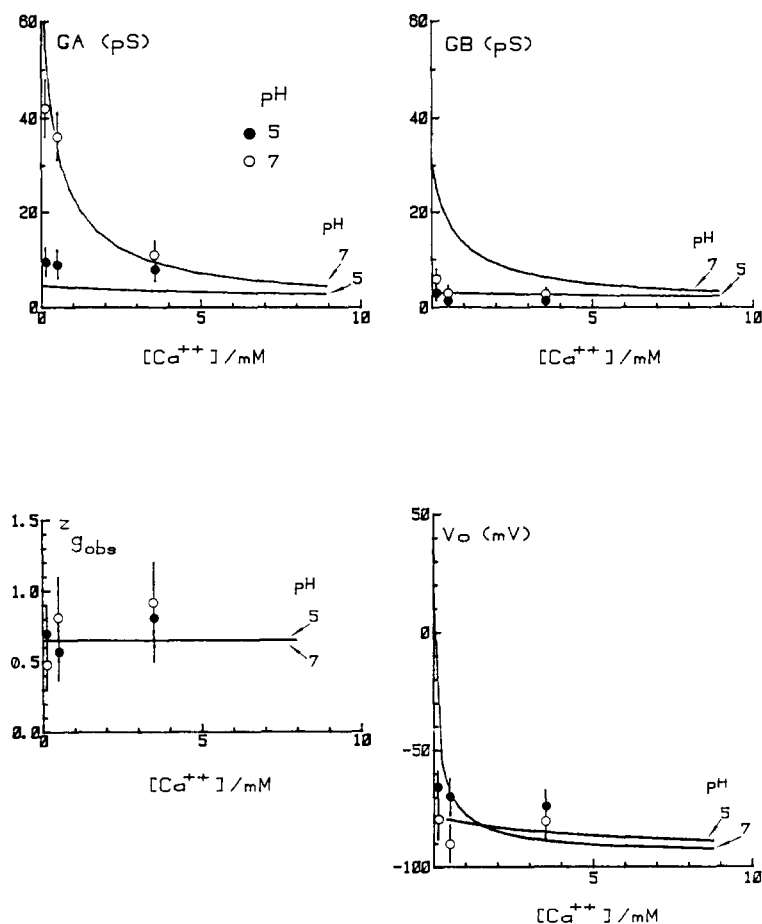


Fig. 10. High and low asymptotes, G_A and inflection point, V_0 , of the instantaneous G/V curve of the hemocyanin channel as a function of the activity of Ca^{2+} added to a 10 mM K_2SO_4 solution for two values of the pH. Other experimental conditions as in Fig. 1a. Open and closed symbols are for Buffers A and B, respectively. Solid lines are drawn according to the model presented in the text making use of Eqns. 10 and 17. The new parameters introduced are $pK_{ACa^{2+}}(0) = 2.7$ and $pK_{BCa^{2+}}(0) = 5.4$, the other parameters being the same as given in Figs. 2 and 8.

$K_1(0) = 14.9$; $q_1 = 1.15e$; $pK_{AH^+}(0) = 5.4$; $\delta_A = 0$; $pK_{BH^+}(0) = 6.4$; $\delta_B = -0.25$. The value of $n = 2$ indicates that two protons are bound cooperatively by the site, the affinity constant being 10-times larger in state B than in state A; the site turns out to be located at the surface of the channel in configuration A, since $\delta_A = 0$, while it feels one-fourth of the applied potential in configuration B, the negative sign of δ_B indicating that it is located at the trans side. As shown in Fig. 9, the model predicts correctly the variations of $z_{g,obs}$ and V_0 with the pH of the solution, and without adding any new parameter, also in the control experiments made in KCl or in K_2SO_4 but with a neutral membrane.

To test the consistency of our fitting procedure, we have verified that indeed, for a given set of model parameters, the function $p(V)$ that can be calculated from the two-state model, Eqn. 2, with the approximate values of $z_{g,obs}$ and V_0 obtained

from Eqns. 15 and 16 coincides with the four-state expression given by Eqn. 12, at least within our experimental resolution. Finally, Eqn. 12 can be extended to the case that Ca^{2+} ions also bind to the same site, competing with protons. Assuming that one Ca^{2+} ion saturates the site, which otherwise can bind two protons, we obtain:

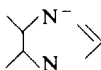
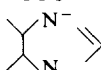
$$\frac{p(V)}{1-p(V)} = K_1 \frac{(1 + \{[H^+]/K_{AH^+}\}^2 + [Ca^{2+}]/K_{ACa^{2+}})}{(1 + \{[H^+]/K_{BH^+}\}^2 + [Ca^{2+}]/K_{BCa^{2+}})} \quad (17)$$

Fig. 10, lower part, shows that just introducing two new parameters, i.e., the dissociation constants $K_{ACa^{2+}}(0)$ and $K_{BCa^{2+}}(0)$, the model can predict consistently also the values of $z_{g,obs}$ and V_0 found in the experiments at different Ca^{2+} concentrations. In the course of this discussion we have introduced a number of dissociation con-

TABLE II

CHEMICAL NATURE OF THE BINDING SITES ON THE HEMOCYANIN CHANNEL

Comparison between the affinities for protons and calcium ions of different sites. Upper part: pK values for the binding of H^+ and Ca^{2+} to various functional groups which are commonly found on proteins. Middle part: pK values for the binding of protons (two groups have been distinguished) and calcium ions to hemocyanins from different species. Lower part: pK values for the binding of H^+ and Ca^{2+} to the sites on *M. crenulata* hemocyanin as obtained in this work studying the instantaneous G/V curves. The first three rows are best-fit parameters obtained using the four-state electrostatic model presented in this work; for the meaning of the symbols see the text. The last two rows are the best values we have found using the three-barrier two-site model (TBM) proposed by Cecchi et al. [5] and refer to sites 1 and 2, respectively.

		pK_{H^+}	$pK_{Ca^{2+}}$	Ref.
Functional group	$-O^-$	7.2	1.5	14, 30
	$-S^-$	8.4	—	
		6.0	—	
	$-COO^-$	2.4	1.3	
	$(-COO^-)_2$	4.3	3.0	
<i>Jasus Edwardsii</i> hemocyanin	$-COO^-$	3.6	—	26
		6.3	—	
<i>Levantina Hierosolima</i> hemocyanin		—	1.9	32
<i>Panulirus interruptus</i> hemocyanin		—	3–3.7	33
<i>M. crenulata</i> hemocyanin	G_A, G_B	5.4	2.4	
	$z_{g,obs}, V_0$ A	5.4	2.7	
	B	6.4	5.4	
TBM	site 1	5	4.5	
	site 2	6.3	2.3	

stants from the channel: three for protons and three for calcium ions. The values we have found for these constants, fitting our model to the experimental data, are reported in Table II and compared to dissociation constants of the same ions from different functional groups which are commonly found on proteins [30]. Our values are consistent with the involvement of carboxyl groups and/or imidazolium ions of histidines in the chemical composition of the binding sites. This interpretation is reinforced by comparison of the pK values found for the binding of protons to these two groups on a hemocyanin molecule, measured by potentiometric titration [26]; our data are indeed intermediate between the two, indicating the probable involvement of both groups. They are also consistent with the finding that chemical modification of histidine residues on *M. crenulata* hemocyanin reduces the conductance of the channel and changes its voltage-dependence [31]. Table II shows also that the dissociation constants for Ca^{2+} ions we have found here are in the range of those measured by other workers on different hemocyanins with various techniques [32,33]. Furthermore, in a previous work, in which chloride salts have been used, we have estimated a stability constant for the binding of Ba^{2+} to the channel which was half that of Ca^{2+} [34], a ratio which is in good agreement with the values measured in a number of organic and inorganic salts of these two divalent cations [35].

A different transport mechanism through the hemocyanin channel has been proposed by Cecchi et al. [5,6] to explain its saturation and selectivity properties. They introduced a three-barrier two-site energy profile of the pore and used the Eyring absolute rate theory to calculate ion transport through it, assuming also single-ion-occupancy and single-file motion. We have used this same model and we have found that, provided one allows for competition between K^+ , H^+ and Ca^{2+} ions for the occupation of the same channel binding sites, it is indeed possible to describe with this model also the I/V curves presented in the present paper. Anyway, this model requires a much larger number of parameters than the one presented here; in fact, the whole energy profile of the pore, eight parameters, has to be redrawn for each different ion and, in addition, at least the values of the two

energy minima and of the central barrier must be adjusted with the electrolyte concentration [5]. A local potential has to be added to these energy values, in order to describe their concentration-dependence, which is almost the same as that introduced in our model by Eqn. 6, and has to be attributed to a local negative charge. Furthermore, from the depth of wells 1 and 2 in the energy profile it is possible to calculate the pK values for the dissociation of the different cations from the two sites of the channel and these values also turned out to be quite similar to those we have found with our model, as shown in Table II. The main conclusions from the two models are hence much the same, but we may notice that the model presented here is also capable of predicting a pH-dependence of the selectivity of the channel between anions and cations (see Table I) which is otherwise not possible using the three-barrier two-site model, at least in the simple form so far presented [5,6]. For these reasons, we feel that the multistate model presented in this work is a valid alternative to the more classical energy profile description of the channel.

Acknowledgements

We are grateful to Ms. M.T. Giunta for her excellent work in typing this manuscript. This research was supported in part by the Italian Ministero di Pubblica Istruzione and Consiglio Nazionale delle Ricerche.

References

- 1 Pant, H.C. and Conran, P. (1972) *J. Membrane Biol.* 8, 357–362
- 2 Alvarez, O., Diaz, E. and Latorre, R. (1975) *Biochim. Biophys. Acta* 389, 444–448
- 3 Pasquali, F. and Menestrina, G. (1985) *Eur. Biophys. J.* 12, 33–41
- 4 McIntosh, T.J., Robertson, J.D., Ting-Beall, H.P., Walter, A. and Zampighi, G. (1980) *Biochim. Biophys. Acta* 601, 289–301
- 5 Cecchi, X., Alvarez, O. and Latorre, R. (1981) *J. Gen. Physiol.* 78, 657–681
- 6 Cecchi, X., Latorre, R. and Alvarez, O. (1984) *J. Membrane Biol.* 77, 277–284
- 7 Menestrina, G. and Antolini, R. (1982) *Biochim. Biophys. Acta* 688, 673–684
- 8 Menestrina, G. (1983) *Biophys. Struct. Mech.* 10, 143–168
- 9 Lindemann, B. (1982) *Biophys. J.* 39, 15–22

- 10 Benz, R., Janko, K. and Läuger, P. (1979) *Biochim. Biophys. Acta* 551, 238–247
- 11 Benz, R., Tokunaga, H. and Nakae, T. (1984) *Biochim. Biophys. Acta* 769, 348–356
- 12 Spray, D.C., Harris, A.L. and Bennet, M.V.L. (1981) *Science* 211, 712–715
- 13 Spray, D.C., Stern, J.H., Harris, A.L. and Bennet, M.V.L. (1982) *Proc. Natl. Acad. Sci. USA* 79, 441–445
- 14 Kostyuk, P.G., Mironov, S.L. and Doroshenko (1982) *J. Membrane Biol.* 70, 181–189
- 15 Mueller, P. and Rudin, D.O. (1968) *Nature* 217, 713–719
- 16 Cecchi, W., Bull, R., Franzoy, R., Coronado, R. and Alvarez, O. (1982) *Biochim. Biophys. Acta* 693, 173–176
- 17 Ehrenstein, G. and Lecar, H. (1977) *Q. Rev. Biophys.* 10, 1–34
- 18 Läuger, P. (1985) *Biophys. J.* 47, 581–591
- 19 Bockris, J.O.M. and Reddy, A.K.N. (1970) *Modern Electrochemistry*, Vol. 1, Plenum Press, New York
- 20 Pitzer, K.S. (1979) in *Activity Coefficients in Electrolyte Solutions* (Pytkowicz, R.M., ed.), Vol. 1, pp. 158–208, CRC Press, Boca Raton
- 21 Delville, A., Gilboa, H. and Laszlo, P. (1982) *J. Chem. Phys.* 77, 2045–2050
- 22 Delville, A. (1984) *Biophys. Chem.* 19, 183–189
- 23 Richards, E.G. (1980) *An Introduction to the Physical Properties of Large Molecules in Solution*, Cambridge University Press, New York
- 24 Pitzer, K.S. (1977) *Acc. Chem. Res.* 10, 371–377
- 25 Brooks, B. and Karplus, M. (1985) *Proc. Natl. Acad. Sci. USA* 82, 4995–4999
- 26 Ellerton, H.D., Blazey, N.D. and Robinson, H.A. (1977) *Biochim. Biophys. Acta* 459, 140–150
- 27 Schultz, S.G. (1980) *Basic Principles of Membrane Transport*, Cambridge University Press, New York
- 28 Hanke, W. and Miller, C. (1983) *J. Gen. Physiol.* 82, 25–45
- 29 Porcelluzzi, C. (1984) *Tesi di laurea, Università degli studi di Trento, Trento*
- 30 Martell, A.E. and Smith, R.M. (1977) *Critical Stability Constants*, Plenum Press, New York
- 31 Griffin, M.C.A. and Sattelle, D.B. (1983) *Biochim. Biophys. Acta* 727, 56–62
- 32 Klarman, A., Shalkai, N. and Daniel, E. (1972) *Biochim. Biophys. Acta* 257, 150–157
- 33 Andersson, T., Chiancone, E. and Forsen, S. (1982) *Eur. J. Biochem.* 125, 103–108
- 34 Menestrina, G. and Antolini, R. (1981) *Period. Biol.* 83, 166–70
- 35 Phillips, C.S.G. and Williams, R.J.P. (1966) *Inorganic Chemistry*, Vol. 2, pp. 81–82, Oxford University Press, Oxford